# Band Offset Enhancement of a-Al$_2$O$_3$/Tensile-Ge for High Mobility Nanoscale pMOS Devices

Michael B. Clavel, *Student Member*, *IEEE*, Mantu K. Hudait, *Senior Member*, *IEEE*

*Abstract*—**The band alignment properties of amorphous Al$_2$O$_3$ on strain-engineered biaxial tensile-strained epitaxial Ge, grown *in-situ* by molecular beam epitaxy on In$_x$Ga$_{1-x}$As virtual substrates, are presented. X-ray photoelectron spectroscopy investigation demonstrated an increase in the valence band offset of the Al$_2$O$_3$/strained Ge system with increasing tensile strain. For Ge strain-states of 1.14%, 1.6%, and 1.94%, the corresponding valence band offsets were found to be 4.43 ± 0.1 eV, 3.95 ± 0.1 eV, and 4.55 ± 0.1 eV, respectively, demonstrating a ~0.8 eV increase as compared to Ge grown on GaAs. The observed enhancement in the valence band discontinuity between tensile-strained Ge and Al$_2$O$_3$ offers a unique and novel path for the simultaneous improvement of hole mobility (*via* strain) and hole confinement (*via* a larger valence band offset) in future low-power and high-performance Ge-based nanoscale pMOS devices.**

*Index Terms*—**Energy band alignment, Al$_2$O$_3$, strained Ge, x-ray photoelectron spectroscopy (XPS).**

## I. INTRODUCTION

CONTINUATION of the aggressive reduction in silicon (Si) complimentary metal-oxide-semiconductor (CMOS) technology has revealed fundamental physical limitations for future Si device scaling. To overcome these challenges, new channel materials and device architectures offering improved drive current, lower operating voltage, and steep sub-threshold dynamics are being extensively investigated [1]–[3]. Among the potential candidates for extending CMOS beyond 10 nm, germanium (Ge) has attracted much attention due to its low band gap, high carrier mobility, and process compatibility with current CMOS process technology [4]. In particular, strained Ge has been investigated for use as the channel material in future high performance [5], [6] and low-power [7] logic, as well as the gain medium in on-Si, group IV-based photonics [8], [9]. However, little attention has been devoted to strain-induced modification of the oxide/semiconductor band alignment [10], [11], essential in evaluating channel carrier confinement.

*In this letter*, we report on the effective modulation of the band alignment between amorphous (a) Al$_2$O$_3$ and biaxial tensile-strained (ε) Ge epilayers grown on In$_x$Ga$_{1-x}$As stressors. Moreover, we demonstrate that the contribution to the band alignment enhancement reflects the combined effects of the ε-Ge strain-state and the intrinsic band discontinuities between ε-Ge and the underlying strain template.

## II. EXPERIMENTAL

In this study, 15 nm - 30 nm thick epitaxially strained Ge layers were grown *in-situ* on In$_x$Ga$_{1-x}$As virtual substrates (VS) utilizing solid-source molecular beam epitaxy (MBE). Strain modulation within the Ge epilayers was achieved by modification of the indium (In) alloy composition in the VS. Three In compositions were selected in order to investigate the effects of varying biaxial tensile strain on the band alignment between ε-Ge and a-Al$_2$O$_3$, specifically: (i) In$_{0.18}$Ga$_{0.82}$As (1.14% ε), (ii) In$_{0.24}$Ga$_{0.76}$As (1.6% ε), and (iii) In$_{0.29}$Ga$_{0.71}$As (1.94% ε). Full details regarding the growth and materials characterization (and associated methodologies) of the Ge/(In)GaAs heterostructures are reported elsewhere [7], [12].

Subsequently, 1.5 nm and 10 nm a-Al$_2$O$_3$ films were deposited at 200°C by atomic layer deposition (ALD) using trimethylaluminum and deionized H$_2$O. Prior to oxide deposition, all samples were stripped of native oxide in dilute HF for 60 s. Immediately following Al$_2$O$_3$ ALD, the samples were transferred to a PHI Quantera SXM x-ray photoelectron spectroscopy (XPS) system for band alignment characterization following the methods described in [7], [12]. A low-energy electron flood gun was utilized to compensate oxide electron loss during spectral acquisition and minimize positive charge accumulation on the sample surface. Statistical deviation in the Au 4f$_{7/2}$ core level binding energy of a Au standard was used to derive an experimental uncertainty of ±0.04%, with subsequent uncertainty estimated using a root sum square approach.

Additionally, in order to broaden the applicability of the measured band alignment data to n- *and* pMOS devices, strain-dependent calculations of the Ge band edges were performed following the deformation potential theory approach described in [13] using the material parameters listed in Table I.

## III. RESULTS AND DISCUSSION

Previous nonlocal pseudopotential calculations [14] of the strained Ge band structure have revealed a crossover point, ε ≈

### TABLE I
#### GERMANIUM MATERIAL PARAMETERS

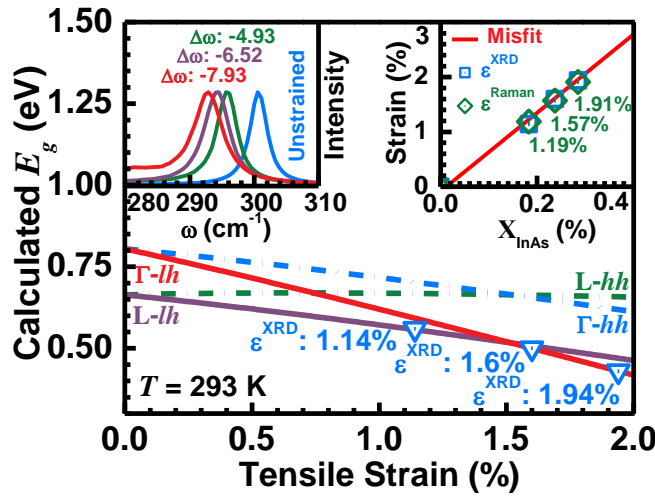| Quantity | Symbol | Units | Value[Ref.] |
|---|---|---|---|
| **Lattice Constant** | $a_0$ | Å | 5.658[15] |
| **Elastic Constants** | $c_{11}$ | 10$^{11}$ dyn/cm$^2$ | 12.60[15] |
| | $c_{12}$ | 10$^{11}$ dyn/cm$^2$ | 4.40[15] |
| | $c_{44}$ | 10$^{11}$ dyn/cm$^2$ | 6.77[15] |
| **Deformation Potentials** | $a$ | eV | -9.48[16] |
| | $b$ | eV | -2.86[17] |
| | $\Xi_d + \frac{1}{3}\Xi_u$ | eV | -2.36[17] |
| **Direct Gap** | $E_g^\Gamma$ | eV | 0.805[13] |
| **Indirect Gap** | $E_g^L$ | eV | 0.664[13] |
| **Spin-Orbit Splitting** | $\Delta_{SO}$ | eV | 0.296[14] |

Fig. 1. Calculated 293 K bandgap-strain dependence for Ge using deformation potential theory [13] and the material parameters found in [13]–[17]. Symbols (blue) represent the expected bandgap value for the strain-states studied in this work. Right inset illustrates the experimental Raman wavenumber shift with increasing Ge strain. Left inset shows the experimental Ge epilayer strain independently determined *via* x-ray diffraction and Raman spectroscopy.

1.5%, at which the Γ-valley minimum supersedes the L-valley minimum as the lowest conduction band (CB) edge. As a result, the L-valley carrier population in ε-Ge is expected to reduce for strain states approaching ε ≈ 1.5%. To account for this change, the bandgap for the lowest CB minimum (at a given ε) is most appropriate when determining the conduction band offset ($\Delta E_C$) at the $Al_2O_3$/ε-Ge heterointerface. Fig. 1 shows the dependence of the calculated 293 K Ge bandgap on the magnitude of the in-plane biaxial tensile strain. As can be seen in Fig. 1, a crossover in the Γ- and L-valley band edges was indeed observed at ε = 1.52%. Congruently, employing the experimental Ge epilayer strain determined *via* Raman spectroscopy (Fig. 1 right inset) and x-ray diffraction analysis (Fig. 1 left inset), the calculated bandgaps for the 1.14%, 1.6%, and 1.94% ε-Ge were 0.56 eV (L-*lh*), 0.50 eV (Γ-*lh*), and 0.43 eV (Γ-*lh*), respectively.

Fig. 2 shows representative XPS spectra recorded from the moderately strained (1.14%) a-$Al_2O_3$/ε-Ge heterointerface, including: (a) the Al 2p core level (CL) and valence band maxima (VBM) from 10 nm a-$Al_2O_3$ deposited on 1.14% ε-Ge; (b) the Ge 3d CL and VBM from the 1.14% ε-Ge epilayer; and (c) the Al 2p and Ge 3d CLs from 1.5 nm a-$Al_2O_3$ deposited on 1.14% ε-Ge. The valence band offset ($\Delta E_V$) can be determined using the method proposed by Kraut *et al.* [18] in conjunction with the measured CL and VBM binding energies, *i.e.*:

$$\Delta E_V = \left( E_{Al2p}^{Al_2O_3} - E_{VBM}^{Al_2O_3} \right) - \left( E_{Ge3d}^{\varepsilon-Ge} - E_{VBM}^{\varepsilon-Ge} \right) - \Delta CL(i) \quad (1)$$

where $E_{Al2p}^{Al_2O_3}$ and $E_{Ge3d}^{\varepsilon-Ge}$ are the CL binding energies for a-$Al_2O_3$ and Ge, respectively, $E_{VBM}$ is the VBM for each material, and $\Delta CL(i)$ is the binding energy separation between the interfacial Al 2p and Ge 3d CLs, *i.e.* $E_{Al2p}^{Al_2O_3} - E_{Ge3d}^{\varepsilon-Ge}$. Linear regression of the onset of valence band emission was used to determine $E_{VBM}$ for each material [7], [12]. Similarly, the experimental a-$Al_2O_3$ band gap, $E_g^{Al_2O_3}$, was extracted from a linear fitting of the O 1s loss spectra [19], [20]. Using the measured values for $\Delta E_V$ and $E_g^{Al_2O_3}$, the conduction band offset



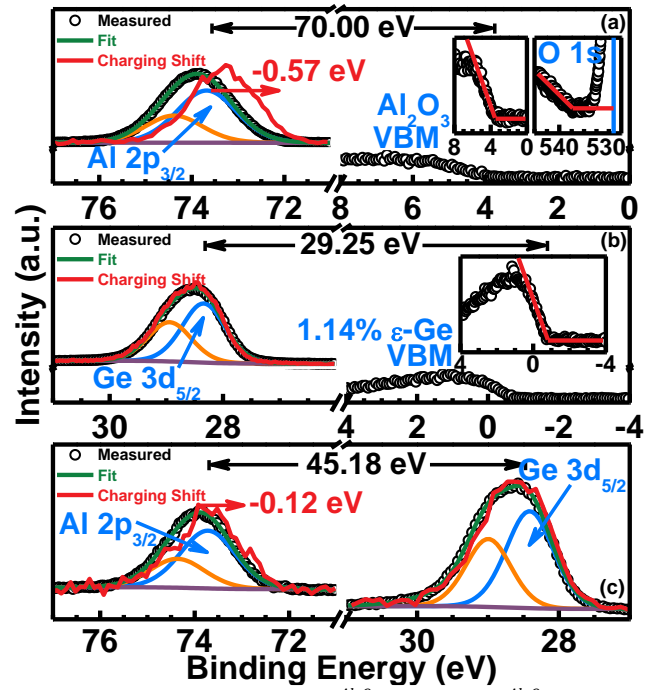Fig. 2. XPS spectra of (a) Al 2p CL ($E_{Al2p}^{Al_2O_3}$) and VBM ($E_{VMB}^{Al_2O_3}$) from the 10 nm $Al_2O_3$/ε-Ge sample, (b) Ge 3d CL ($E_{Ge3d}^{\varepsilon-Ge}$) and ε-Ge VBM ($E_{VBM}^{\varepsilon-Ge}$) from the ε-Ge virtual substrate, and (c) Ge 3d ($E_{Ge3d}^i$) and Al 2p ($E_{Al2p}^i$) from the 1.5 nm $Al_2O_3$/ε-Ge interface for the 1.14% tensile strain $Al_2O_3$/ε-Ge structure.

($\Delta E_C$) was calculated by [7], [12], [20]:

$$\Delta E_C = E_g^{Al_2O_3} - E_g^{\varepsilon-Ge} + \Delta E_V \quad (2)$$

where $E_g^{\varepsilon-Ge}$ is the band gap energy of ε-Ge. Following the procedures defined above and using the calculated $E_g^{\varepsilon-Ge}$ at each strain state, the band discontinuities for each a-$Al_2O_3$/ε-Ge heterointerface were determined, as summarized in Table II.

It is important to note that the band offset values presented in Table II are sensitive to several charging mechanisms commonly observed in XPS analysis, including x-ray irradiation and/or a built-in potential within the oxide/semiconductor heterostructure. These mechanisms serve to modify the energy of the escaping photoelectron, resulting in a shift of the measured binding energy due to an effective accumulation of charge within the sample [21]. To examine the impact of such modifications on the oxide/semiconductor band alignment, the CL spectra shown in Fig. 2 are presented both before (green) and after (red) saturation of the sample surface by way of extended x-ray beam exposure. A maximum charging-induced shift, $E_{ch}$, of 0.57 ± 0.04 eV was observed for

TABLE II
SUMMARY OF THE MEASURED AND CALCULATED XPS DATA FROM THE
$Al_2O_3$/ε-GE HETEROSTRUCTURES INVESTIGATED IN THIS WORK

| Structure | Measured $Al_2O_3$ $E_g$ (eV) | Calculated ε-Ge $E_g$ (eV) | Measured $\Delta E_V$ (eV) | Calculated $\Delta E_C$ (eV) |
|---|---|---|---|---|
| $Al_2O_3$/1.14% ε-Ge | 6.59 ± 0.04 | 0.56 (L-valley) | 4.43 ± 0.1 | 1.6 ± 0.1 |
| $Al_2O_3$/1.6% ε-Ge | 6.79 ± 0.04 | 0.50 (Γ-valley) | 3.95 ± 0.1 | 2.34 ± 0.1 |
| $Al_2O_3$/1.94% ε-Ge | 6.78 ± 0.04 | 0.43 (Γ-valley) | 4.55 ± 0.1 | 1.8 ± 0.1 |
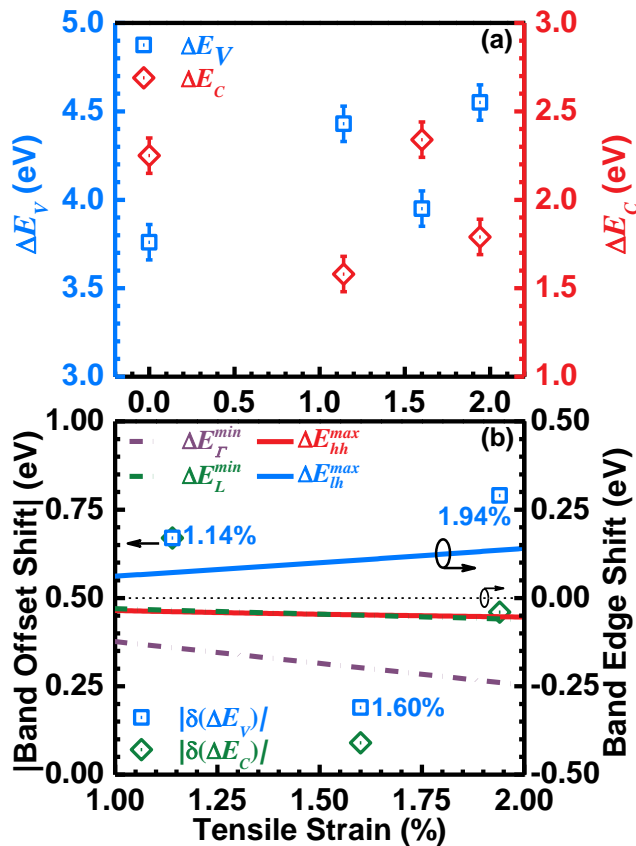
Fig. 3.  (a) Experimental valence band ($\Delta E_V$) and calculated conduction band ($\Delta E_C$) offsets for the a-Al$_2$O$_3$/ε-Ge system studied in this work as well as a-Al$_2$O$_3$/Ge/GaAs. (b) Comparison of the shift in energy band edge due to strain and the magnitude of the experimental band offset shifts with respect to the unstrained a-Al$_2$O$_3$/Ge/GaAs heterostructure.

the Al $2p_{3/2}$ CL recorded from the 10 nm Al$_2$O$_3$/1.14% ε-Ge sample, decreasing to 0.12 ± 0.04 eV for the ultra-thin 1.5 nm Al$_2$O$_3$ oxide on the same structure. As can be seen in Figs. 2b and 2c, no predominant shift in the Ge $3d_{5/2}$ CL binding energy was observed, indicating an asymmetric accumulation of charge within the Al$_2$O$_3$/1.14% ε-Ge structure that strongly depends on oxide thickness. Recent results [22] suggest that the formation of gap states on the Al$_2$O$_3$ surface modifies the Al$_2$O$_3$ charge neutrality level, CNL$^{Al_2O_3}$, raising it above the charge neutrality level of Ge, CNL$^{Ge}$, and resulting in electron transfer from Ge to Al$_2$O$_3$. The manifestation of this charge transfer would be a shift in the measured CLs to lower binding energies, which can indeed be observed in Figs. 2a and 2c. These results suggest that encapsulation of the oxide surface, *e.g.*, *via* the deposition of < 10 Å of metal, may enhance accuracy when investigating practical MOS gate structures. Nevertheless, for this work, the measured CLs for each material were compensated using the observed $E_{ch}$ in order to provide a more representative view of the Al$_2$O$_3$/ε-Ge band alignment.

Fig. 3a shows the empirical and calculated band offset parameters for the a-Al$_2$O$_3$/ε-Ge structures considered in this study in addition to the measured band offsets of a-Al$_2$O$_3$ deposited on Ge grown on GaAs. Similarly, Fig. 3b highlights the magnitude of the a-Al$_2$O$_3$/ε-Ge band offset shifts with respect to the a-Al$_2$O$_3$/Ge/GaAs heterostructure in comparison to the calculated band edge shifts at the Γ- and L-valley CB

(purple, green) and heavy- and light-hole VBM (red, blue) for increasing strain. As can be seen from Fig. 3a, $\Delta E_V$ (blue, symbol) demonstrated a positive trend with respect to the tensile strain in the Ge epilayer. Moreover, the magnitude of the enhancement in $\Delta E_V$ (~0.8 eV, Fig. 3b) for the highly strained (1.94% ε) structure was found to be larger than the Ge band gap, suggesting a combined influence on the a-Al$_2$O$_3$/ε-Ge band alignment from both the strain-state of the epitaxial Ge as well as the underlying ε-Ge/In$_x$Ga$_{1-x}$As band discontinuities. The observed shift in $\Delta E_V$ was found to differ from similar structures grown on GeSn- [10] and SiGe-based [11] strain templates, thus suggesting fundamentally different roles in interface band structure modification between III-V- and group IV-based pseudomorphic templates. Whereas modification of the oxide/ε-Ge band alignment for group IV-based virtual substrates favors strain-induced band gap reduction, III-V-based strain templates appear to leverage both larger intrinsic IV/III-V band discontinuities [7], [23] as well as strain-related band structure alterations in the pseudomorphic Ge layer.

Lastly, it can be posited that the higher strain-states investigated in this work also play a role in the increased strain-dependency of the a-Al$_2$O$_3$/ε-Ge band offsets. In this regard, the increased surface energy of the highly strained Ge epilayer alters the near-interfacial O-O interaction in a-Al$_2$O$_3$. Note that the valence band (VB) electron states in metal oxides are derived from the 2p states of the O anions [24]. Accordingly, strain-related modification of the O-O interaction in near-interfacial a-Al$_2$O$_3$ could result in associated changes in the a-Al$_2$O$_3$ VB structure, and thus a lowering of the a-Al$_2$O$_3$ VBM (*i.e.*, an increase in $\Delta E_V$) [25]. Thus, the incorporation of increased strain into Ge films grown on III-V stressors may offer several advantages for the design of ε-Ge-based *p*-channel field-effect transistors, including additional enhancement to channel hole confinement as well as improved hole mobilities.

## IV. CONCLUSION

The effect of biaxial tensile strain on the energy band discontinuities between a-Al$_2$O$_3$ and epitaxial ε-Ge was systematically investigated. The valence band offset, $\Delta E_V$, was found to reflect strain-dependent and heterostructural (ε-Ge/In$_x$Ga$_{1-x}$As) enhancements. Moreover, a significant increase in $\Delta E_V$, up to ~0.8 eV, was observed for a-Al$_2$O$_3$ deposited on 1.94% ε-Ge (4.55 ± 0.1 eV) as compared to unstrained a-Al$_2$O$_3$/Ge/GaAs (3.76 ± 0.1 eV). The ability to substantially augment $\Delta E_V$ *via* tensile strain suggests an approach to reduce gate leakage current, and therefore power dissipation, in future ε-Ge-based pMOS technology. In conjunction with strain-induced hole mobility enhancement, the provided band alignment parameters offer an exciting and innovative direction for realizing ε-Ge devices with high drive currents, reduced gate leakage, and flexibility in device application.

## REFERENCES

[1] A. M. Ionescu and H. Riel, "Tunnel field-effect transistors as energy-efficient electronic switches," *Nature*, vol. 479, no. 7373, pp. 329–337, Nov. 2011. DOI:10.1038/nature10679

[2] A. C. Seabaugh and Q. Zhang, "Low-voltage tunnel transistors for beyond CMOS logic," *Proc. IEEE*, vol. 98, no. 12, pp. 2095–2110, Dec. 2010. DOI: 10.1109/JPROC.2010.2070470

[3] M. Heyns, A. Alian, G. Brammertz, M. Caymax, Y.C. Chang, L.K. Chu, B. De Jaeger, G. Eneman, F. Gencarelli, G. Groeseneken, G. Hellings, A. Hikavyy, T.Y. Hoffmann, M. Houssa, C. Huyghebaert, D. Leonelli, D. Lin, R. Loo, W. Magnus, C. Merckling, M. Meuris, J. Mitard, L. Nyns, T. Orzali, R. Rooyackers, S. Sioncke, B. Soree, X. Sun, A. Vandooren, A.S. Verhulst, B. Vincent, N. Waldron, G. Wang, W.E. Wang, and L. Witters, "Advancing CMOS beyond the Si roadmap with Ge and III/V devices," in *Proc. IEEE Int. Electron Devices Meeting (IEDM)*, Washington, DC, USA, 2011, pp. 13.1.1–13.1.4. DOI: 10.1109/IEDM.2011.6131543

[4] P. D. Nguyen, M. Clavel, P. S. Goley, J.-S. Liu, N. P. Allen, L. J. Guido, and M. K. Hudait, "Heteroepitaxial Ge MOS devices on Si using composite AlAs/GaAs buffer," *IEEE J. Electron Devices Soc.*, vol. 3, no. 4, pp. 341–348, July 2015. DOI: 10.1109/JEDS.2015.2425959

[5] S. Gupta, V. Moroz, L. Smith, Q. Lu, and K. C. Saraswat, "A group IV solution for 7 nm FinFET CMOS: Stress engineering using Si, Ge, and Sn," in *Proc. IEEE Int. Electron Devices Meeting (IEDM)*, Washington, DC, USA, 2013, pp. 26.3.1–26.3.4. DOI: 10.1109/IEDM.2013.6724696

[6] A. Agrawal, M. Barth, G. B. Rayner Jr., Arun V. T., C. Eichfeld, G. Lavallee, S.-Y. Yu, X. Sang, S. Brookes, Y. Zheng, Y.-J. Lee, Y.-R. Lin, C.-H. Wu, C-H. Ko, J. LeBeau, R. Engel-Herbert, S. E. Mohney, Y.-C. Yeo, and S. Datta, "Enhancement mode strained (1.3%) germanium quantum well FinFET ($W_{Fin}$=20nm) with high mobility ($\mu_{Hole}$=700 cm$^2$/Vs), low EOT (~0.7nm) on bulk silicon substrate," in *Proc. IEDM Tech. Dig.*, San Francisco, CA, USA, 2014, pp. 16.4.1–16.4.4. DOI: 10.1109/IEDM.2014.7047064

[7] M. Clavel, P. Goley, N. Jain, Y. Zhu, and M. K. Hudait, "Strain-engineered biaxial tensile epitaxial germanium for high-performance Ge/InGaAs tunnel field-effect transistors," *IEEE J. Electron Devices Soc.*, vol. 3, no. 3, pp. 184–193, May 2015. DOI: 10.1109/JEDS.2015.2394743

[8] R. Soref, "The past, present, and future of silicon photonics," *IEEE J. Sel. Top. Quantum Electron.*, vol. 12, no. 6, pp. 1678–1687, Nov. 2006. DOI: 10.1109/JSTQE.2006.883151

[9] Y. Cai, Z. Han, X. Wang, R. E. Camacho-Aguilera, L. C. Kimerling, J. Michel, and J. Liu, "Analysis of threshold current behavior for bulk and quantum-well germanium laser structures," *IEEE J. Sel. Top. Quantum Electron*, vol. 19, no. 4, pp. 1901009, Feb. 2013. DOI: 10.1109/JSTQE.2013.2247573

[10] H.-Y. Chou, V. V. Afanas'ev, M. Houssa, A. Stesmans, B. Vincent, F. Gencarelli, Y. Shimura, C. Merckling, R. Loo, O. Nakatsuka, and S. Zaima, "Band alignment at interfaces of amorphous $Al_2O_3$ with $Ge_{1-x}Sn_x$- and strained Ge-based channels," *Appl. Phys. Lett.*, vol. 104, no. 20, pp. 202107–1—202107–5, May 2014. DOI: 10.1063/1.4878558

[11] S. Y. Chiam, W. K. Chim, C. Pi, A. C. H. Huan, S. J. Wang, J. S. Pan, S. Turner, and J. Zhang, "Band alignment of yttrium oxide on various relaxed and strained semiconductor substrates," *J. Appl. Phys.*, vol. 103, no. 8, pp. 083702–1—083702–12, Apr. 2008. DOI: 10.1063/1.2904928

[12] M. Clavel, D. Saladukha, P. S. Goley, T. J. Ochalski, F. Murphy-Armando, R. J. Bodnar, and M. K. Hudait, "Heterogeneously-grown tunable tensile strained germanium on silicon for photonic devices," *ACS Appl. Mater. Interfaces*, vol. 7, no. 48, pp. 26470–26481, Nov. 2015. DOI: 10.1021/acsami.5b07385

[13] J. Menendez and J. Kouvetakis, "Type-I Ge/$Ge_{1-x-y}Si_xSn_y$ strained-layer heterostructures with a direct Ge bandgap," *Appl. Phys. Lett.*, vol. 85, no. 7, pp. 1175–1177, June 2004. DOI: 10.1063/1.1784032

[14] M. V. Fischetti and S. E. Laux, "Band structure, deformation potentials, and carrier mobility in strained Si, Ge, and SiGe alloys," *J. Appl. Phys.*, vol. 80, no. 4, pp. 2234–2252, Aug. 1996. DOI: 10.1063/1.363052

[15] *Handbook Series on Semiconductor Parameters*, World Scientific Publishing Co., Singapore, 1996, pp. 33–58.

[16] C. G. Van de Walle, "Band lineups and deformation potentials in the model-solid theory," *Phys. Rev. B*, vol. 39, no. 3, pp. 1871–1883, Jan. 1989. DOI: 10.1103/PhysRevB.39.1871

[17] M. Chandrasekhar and F. Pollak, "Effects of uniaxial stress on the electroreflectance spectrum of Ge and GaAs," *Phys. Rev. B*, vol. 15, no. 4, pp. 2127–2144, Feb. 1977. DOI: 10.1103/PhysRevB.15.2127

[18] E. A. Kraut, R. W. Grant, J. R. Waldrop, and S. P. Eowalczyk, "Precise determination of the valence-band edge in x-ray photoemission spectra: Application to measurement of semiconductor interface potentials," *Phys. Rev. Lett.*, vol. 44, no. 24, pp. 1620–1623, June 1980. DOI: 10.1103/PhysRevLett.44.1620

[19] H. Itokawa, T. Maruyama, S. Miyazaki, and M. Hirose, "Determination of bandgap and energy band alignment for high-dielectric-constant gate insulators using high-resolution x-ray photoelectron spectroscopy," in *Ext. Abstr. Conf. Solid State Devices Mater.*, Tokyo, Japan, 1999, pp. 158–159. DOI: 10.7567/SSDM.1999.B-4-1

[20] M. K. Hudait, Y. Zhu, D. Maurya, S. Priya, P. K. Patra, A. W. K. Ma, A. Aphale, and I. Macwan, "Structural and band alignment properties of $Al_2O_3$ on epitaxial Ge grown on (100), (110), and (111)A GaAs substrates by molecular beam epitaxy," *J. Appl. Phys.*, vol. 113, no. 13, pp. 134311–1—134311–8, Apr. 2013. DOI: 10.1063/1.4799367

[21] E. Bersch, M. Di, S. Consiglio, R. D. Clark, G. J. Leusink, and A. C. Diebold, "Complete band offset characterization of the $HfO_2$/$SiO_2$/Si stack using charge corrected x-ray photoelectron spectroscopy," *J. Appl. Phys.*, vol. 107, no. 4, pp. 043702–1—043702–13, Feb. 2010. DOI: 10.1063/1.3284961

[22] X. Wang, J. Xiang, W. Wang, C. Zhao, and J. Zhang, "Dependence of electrostatic potential distribution of $Al_2O_3$/Ge structure on Ge thickness," *Surf. Sci.*, vol. 651, pp. 94–99, Apr. 2016. DOI: 10.1016/j.susc.2016.04.001

[23] J.-S. Liu, M. B. Clavel, and M. K. Hudait, "Performance evaluation of novel strain-engineered Ge-InGaAs heterojunction tunnel field-effect transistors," *IEEE Trans. Electron Devices*, vol. 62, no. 10, pp. 3223–3228, Oct. 2015. DOI: 10.1109/TED.2015.2469536

[24] G. Lucovsky, "Correlations between electronic structure of transition metal atoms and performance of high-*k* gate dielectrics in advanced Si devices," *J. Non-Cryst. Solids*, vol. 303, no. 1, pp. 40–49, Feb. 2002. DOI: 10.1016/S0022-3093(02)00962-6

[25] V. V. Afanas'ev, M. Houssa, A. Stesmans, C. Merckling, T. Schram, and J. A. Kittl, "Influence of $Al_2O_3$ crystallization on band offsets at interfaces with Si and $TiN_x$," *Appl. Phys. Lett.*, vol. 99, no. 7, pp. 072103–1—072103–3, Aug. 2011. DOI: 10.1063/1.3623439